Annals of Hematology
https://doi.org/10.1007/s00277-024-05670-7

ORIGINAL ARTICLE

A promising natural product in diffuse large B-cell lymphoma therapy by targeting PIM1

Xinyun Zhang[1,5] · Qi Su[2] · Yuchen Zhang[1] · Rong Rong[3] · Si Chen[4] · Lexin He[4] · Wenzhuo Zhuang[2] · Bingzong Li[1]

Received: 9 October 2023 / Accepted: 14 February 2024

Abstract

Diffuse large B-cell lymphoma (DLBCL) is the most common and aggressive type of B-cell lymphoma. Unfortunately, about one-third of patients either relapse after the initial treatment or are refractory to first-line therapy, indicating a need for new treatment modalities. PIM serine/threonine kinases are proteins that are associated with genetic mutations, overexpression, or translocation events in B-cell lymphomas. We conducted an integrative analysis of whole-exome sequencing in 52 DLBCL patients, and no amplification, mutation, or translocation of the PIM1 gene was detected. Instead, analyses of TCGA and GTEx databases identified that PIM1 expression was increased in DLBCL samples compared to normal tissue, and high expression levels were associated with poor overall survival. Moreover, interference of PIM1 significantly suppressed DLBCL cell proliferation. In addition, we identified anwulignan, a natural small-molecule compound, as a PIM1 inhibitor. Anwulignan directly binds to PIM1 and exerts antitumor effects on DLBCL in vitro and in vivo by inducing apoptosis, cell cycle arrest, and autophagic cell death. Furthermore, we identified an effective synergistic combination between anwulignan and chidamide. Our findings suggested that PIM1 could be a therapeutic target and prognostic factor for DLBCL, and anwulignan holds promise for future development as a natural product for treatment.

Keywords PIM1 · DLBCL · Natural small-molecule compound · c-Myc

Introduction

DLBCL, the most prevalent form of aggressive B-cell lymphoma in adults, displays significant clinical variability and a complex molecular landscape [1, 2]. Although the anti-CD20 monoclonal antibody rituximab in combination with chemotherapy (R-CHOP) is the standard of care for first-line DLBCL treatment, approximately one in three patients relapse after the initial response or are refractory to first-line therapy [3]. This underscores the need for better treatment modalities, including the discovery of novel drugs and targets, to address this challenge. Therefore, there is an urgent need to identify new therapies to improve patient outcomes.

The PIM family of serine/threonine kinases consists of three highly conserved oncogenes (PIM1-3) that are frequently upregulated in diverse solid tumors and hematologic malignancies [4]. PIMs control the functions of proteins involved in various cellular processes, including transcription, translation, the cell cycle, metabolism, survival, and immune evasion [5, 6]. Considerable evidence supports the involvement of PIM1 and PIM2 in DLBCL pathogenesis. Recent studies have identified PIM2 inhibition as a viable therapeutic approach for the treatment of DLBCL. Moreover, PIM1 has been identified as a target for aberrant somatic hypermutations in DLBCL, and multiple studies have demonstrated high protein expression in this malignancy [7]. Consequently, it is important to investigate the potential role of PIM1 in the pathogenesis of DLBCL and assess its potential as a therapeutic target.

✉ Wenzhuo Zhuang
zhuangwenzhuo@suda.edu.cn

✉ Bingzong Li
lbzwz0907@hotmail.com

1 Department of Hematology, the Second Affiliated Hospital of Soochow University, San Xiang Road 1055, Suzhou 215006, China

2 Department of Cell Biology, School of Biology & Basic Medical Sciences, Suzhou Medical College of Soochow University, Ren Ai Road 199, Suzhou 215123, China

3 Department of Biological Sciences, Xi'an Jiaotong-Liverpool University, Suzhou, China

4 Suzhou Sano Precision Medicine Ltd, Suzhou, China

5 Department of Pharmacy, the Second Affiliated Hospital of Soochow University, Suzhou, China

Published online: 01 March 2024

The discovery and development of natural products and their analogs have significantly affected pharmacotherapy, particularly in the treatment of cancer [8, 9]. Many chemotherapeutic agents currently used in cancer treatment are derived from plants, such as paclitaxel (taxol) from Taxus brevifolia (Pacific Yew) and vinblastine and vincristine from the Madagascar periwinkle plant (Catharanthus roseus) [10].

This study aimed to investigate the therapeutic potential of DLBCL, elucidate its underlying mechanism of action, and explore innovative combination treatment strategies for this disease. In this study, three main questions were addressed: (a) Is PIM1 a valuable therapeutic target and a potential prognostic biomarker for DLBCL? (b) Are there any naturally occurring small-molecule compounds that exhibit inhibitory effects on PIM1, thereby indicating their potential as candidate compounds for DLBCL treatment? (c) Is the combination of a PIM inhibitor with drugs currently under preclinical and clinical investigation a potentially promising strategy for enhancing the therapeutic efficacy of DLBCL?

Materials and methods

Cell lines

The SU-DHL-8, SU-DHL-2, and Farage cell lines were cultured in RPMI-1640 medium (Hyclone) supplemented with 10% fetal bovine serum at 37 °C in an atmosphere containing 5% CO_2. These cell lines underwent short tandem repeat (STR) marker analysis by Genetic Testing Biotechnology Corporation (Suzhou, China) to verify their identity.

Cytotoxicity assay

DLBCL cells were seeded into 96-well plates at a density of 10 × 10^4 cells/mL in 90 μL of medium per well. The cells were treated with various concentrations of Anwulignan (1, 10, 25, 50, and 100 μM) for 48 h, with 10 μL of the compound added to each well. After the treatment period, 10 μL of CCK-8 kit reagent was added to each well and incubated at 37 °C for 2 h. The absorbance at 450 nm was measured using a microplate reader to determine the final cell viability.

Data acquisition

Gene expression profiles for DLBCL were obtained from The Cancer Genome Atlas (TCGA) dataset, which included 48 samples. The TCGA dataset was accessed through the following website: https://portal.gdc.cancer.gov/. Normal control datasets for DLBCL were obtained from the Genotype-Tissue Expression (GTEx) dataset, which included 337 samples. The GTEx dataset was accessed through the following website: https://www.gtexportal.org.

Ethics statement and clinical specimens

This study was conducted by the Declaration of Helsinki and approved in accordance with Ethics Committee of Soochow University Union Hospital. Written informed consent was obtained from all patients, and all experiments were performed in compliance with relevant regulations. A total of 52 DLBCL tissue samples were collected from The Second Affiliated Hospital of Soochow University and frozen in liquid nitrogen for further analysis. DLBCL cases were confirmed by pathological examination of lymph node biopsy or lymphadenectomy according to the 2017 WHO Classification of Lymphoid Neoplasms.

Transcriptome RNA sequencing

SU-DHL-8 cells were treated with anwulignan (60.55 μM) and a normal control group was also established. The relevant indexes were measured 12 h after treatment. Total RNA was extracted from the cells and quantified, and eukaryotic mRNA was enriched using magnetic beads with Oligo (dT) connectors. The mRNA was randomly fragmented into short fragments using Fragmentation Buffer and then used as a template to synthesize the first strand of cDNA with Random hexamers. The second strand of cDNA was synthesized by adding Buffer, dNTPs, RNaseH, and DNA polymerase I. The double-stranded cDNA products were purified using AMPureXP beads, and the sticky ends of the DNA were repaired to blunt ends using T4 DNA polymerase and Klenow DNA polymerase. Adenosine bases and adapters were added to the 3' ends, and the library was selected using AMPureXP beads. PCR amplification was performed to obtain the final sequencing library, which was then sequenced using Illumina Hiseq 6000 after a quality inspection. The transcriptome sequencing was conducted by Suzhou Sano Precision Medicine Ltd. Raw data have been deposited in the Gene Expression Omnibus (GEO) public repository for microarray data (accession number GSE229577 and GSE229896).

DARTS

The DARTS method was utilized to determine the specific protein target of anwulignan based on the protocol described by Lomenick et al. Protein lysates obtained from DLBCL cells were quantified using the bicinchoninic acid protein assay. Anwulignan was then

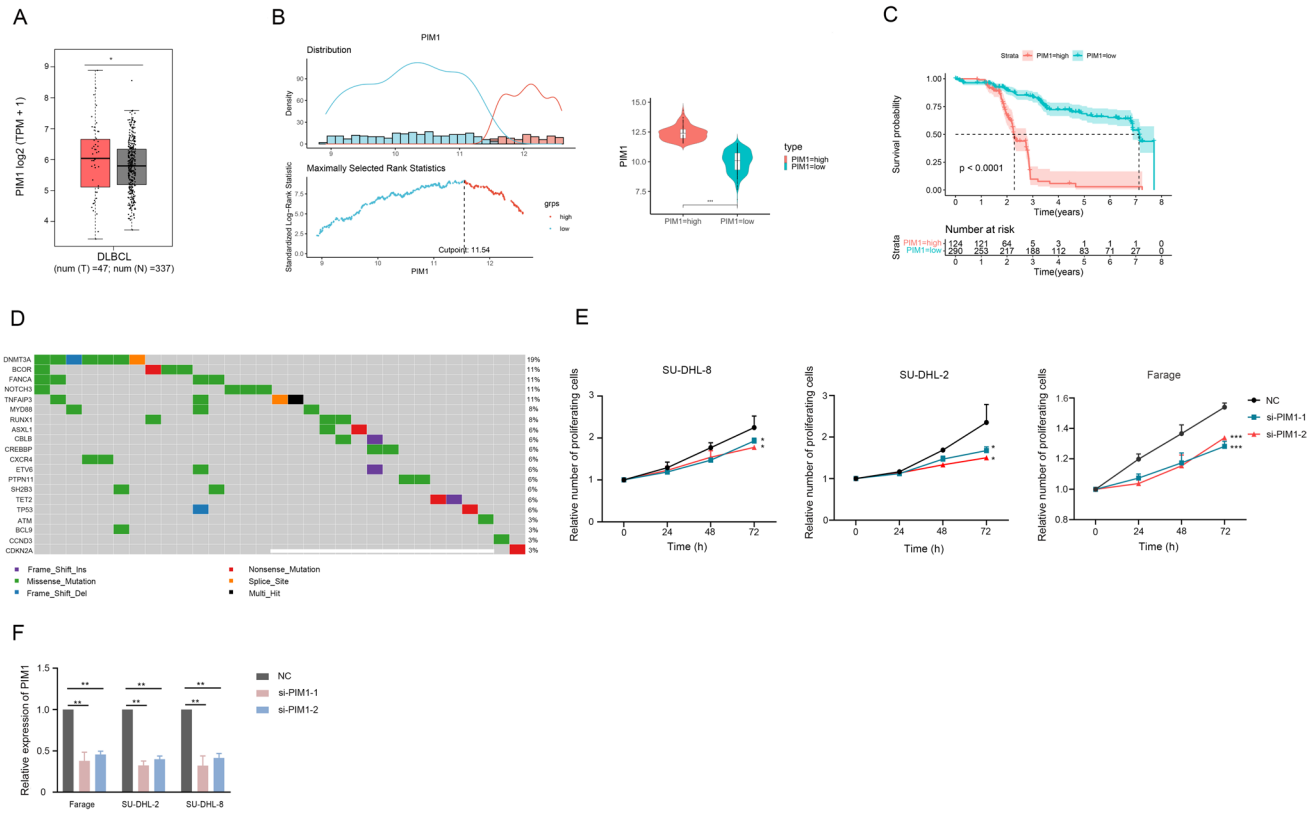

Fig. 1 PIM1 is a potential therapeutic target for DLBCL. **A** The expression of PIM1 in DLBCL patients from the TCGA and GTEx databases. The study comprised 47 DLBCL samples by the color red and 337 normal tissues indicated by gray. **B** The ROC curve analysis determined a cutoff value of 11.54 for high PIM1 expression. **C** Overall survival analysis of PIM1 gene (GSE10846). **D** The mutation patterns of the top 10 most frequently mutated driver genes across 52 DLBCL samples. **E** CCK-8 assay was employed to evaluate cell proliferation following PIM1 interference ($n = 3$). **F** The expression level of PIM1 was detected by qPCR

co-incubated with the lysates at room temperature for 60 min. The drug-protein complex was subjected to proteolysis by pronase (1:50, Roche Applied Science) at room temperature for 10 min. The lysates were then denatured and analyzed through western blotting.

Cellular protein thermal shift assay

The intact-cell protein thermal shift assay was conducted as previously described. SU-DHL-8 cells were treated with either dimethylsulfoxide as control or anwulignan (IC_{50}) for 12 h. Following treatment, the cells were trypsinized and resuspended in phosphate-buffered saline (PBS). The cell suspension was then equally distributed into eight PCR tubes, which were heated to temperatures ranging from 44–52 °C for 3 min and subsequently cooled to room temperature for 3 min. The cells were lysed by three cycles of freeze-thawing using liquid nitrogen, and the lysates were centrifuged at 20,000 g for 20 min to separate the soluble proteins from the precipitates. The supernatants were analyzed by SDS-PAGE followed by western blot using PIM1 antibody to detect the protein thermal shift.

In vivo tumor xenograft model

The animal experiments were conducted according to the institutional guidelines for the use of laboratory animals and after permission was acquired from the Soochow university ethical committee for animal experimentation. Four-week-old female NOD-Scid mice weighing ~10 to 15 g were purchased from Biocytogen Company and fed in the specific pathogen–free barrier system. Mice were subcutaneously injected in the left flank with SU-DHL-8 cells (1×10^6) in 50% Matrigel (Corning). Tumor volume was monitored every other day using electronic digital calipers in 2 dimensions. Tumor volume was calculated using the following formula: tumor volume (mm^3) = (smallest diameter $2 \times$ largest diameter)/2. When tumors were ~100 $mm^3 \pm 10\%$, the mice were randomly

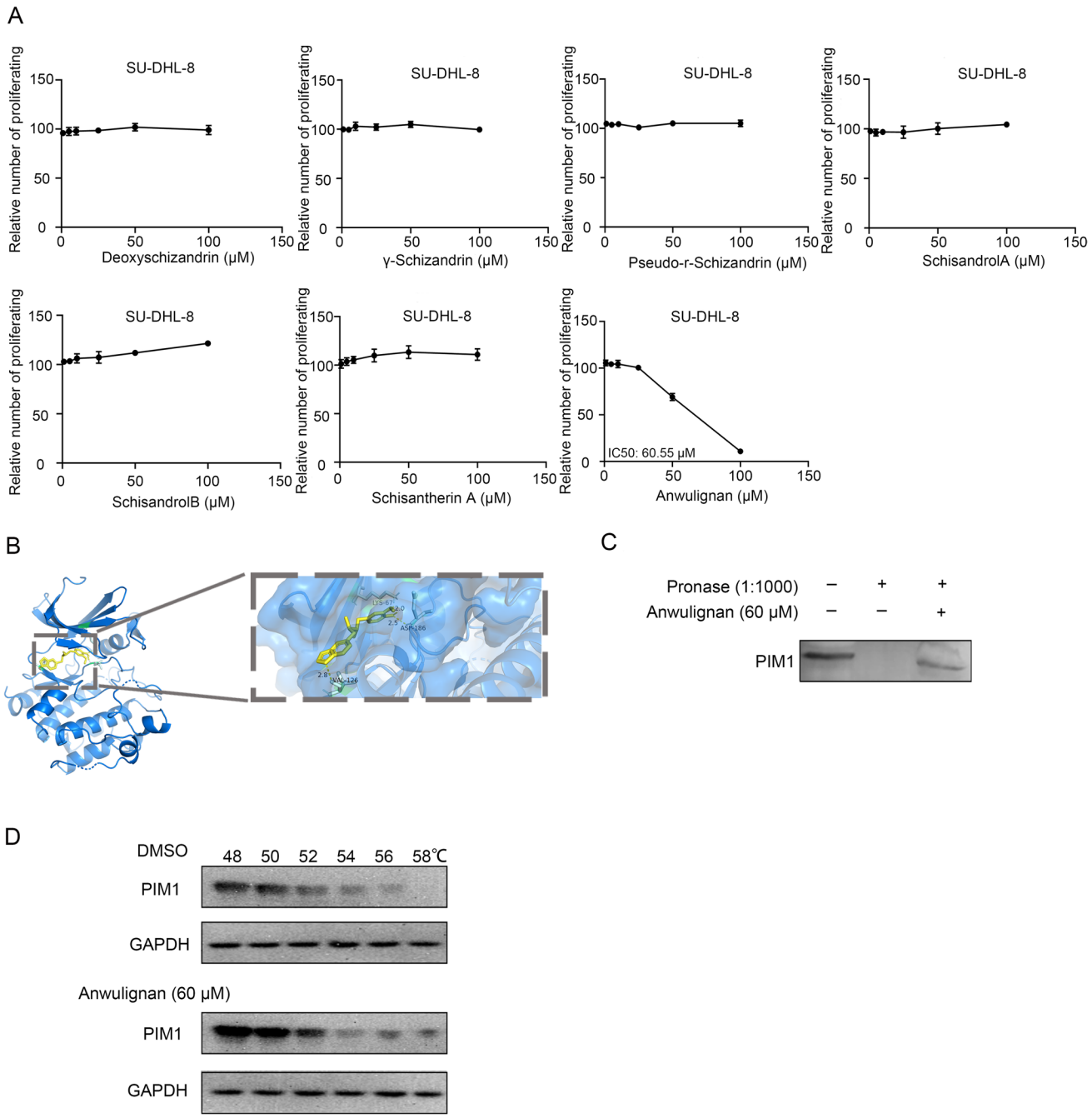

Fig. 2 Candidate compound screening for PIM1. **A** DLBCL cell line (SU-DHL-8) was treated with increasing concentrations of deoxyschizandrin, γ-Schizandrin, pseudo-r-Schizandrin, schisandrolA, schisandrolB, schisantherin A and anwulignan for 48 h respectively and cell viability was measured by CCK8 assay. IC_{50} values in the SU-DHL-8 cell line are shown. **B** Predicted binding modes of anwulignan with PIM1 are illustrated. **C** Lysates from SU-DHL-8 cells were incubated with anwulignan (60 μM) for 12 h, and a final concentration of 0.01% pronase E was added for 30 min. The PIM1 expression was detected by western blot analysis. **D** SU-DHL-8 cells incubated with or without anwulignan (1 μM) for 12 h were subjected to CETSA assay. PIM1 was normalized with actin

divided into 2 groups. One group was intraperitoneally injected with anwulignan (50 mg/kg per day), and the other groups received PBS every other day consecutively for a total of 5 times.

Statistical analysis

To explore the relationship between clinical variables, PIM1 expression measures, and censored outcomes, survival

analysis was conducted using the survival package in R. The primary outcomes of interest were PFS and OS. GraphPad Prism 8 (GraphPad Software, San Diego, CA) was utilized for statistical analysis, and the data was presented in the form of bar graphs with mean ± SD values. An unpaired, two-tailed t-test was performed to compare the two groups, and statistical significance was set at $P < 0.05$.

Results

PIM1 is a potential therapeutic target in DLBCL

Analyses of the TCGA and GTEx databases revealed that PIM1 expression was higher in DLBCL samples than in normal tissues (Fig. 1A). In addition, elevated expression of PIM1 was notably correlated with poor overall survival (OS) outcomes in DLBCL patients, with a calculated ROC curve analysis identifying a cutoff value of 11.54 (Fig. 1B, C). Univariate and multivariate analyses using the Cox risk proportion model revealed a significant association between PIM1 and OS (Table S1). To further evaluate the prognostic significance of PIM1, we tested the Area Under Curve (AUC) index of models fitted with the NCCN-IPI alone and the NCCN-IPI with PIM1. Leave-one-out cross-validation was performed to validate the prognostic value of PIM1. The AUC of the model that included the combination of NCCN-IPI and PIM1 was slightly higher than that of the models without PIM1, indicating that PIM1 improved the prognostic stratification of patients with DLBCL (Table S2). Previous studies have shown that mutations in PIM1 occur in DLBCL [11]. We performed an integrative whole-exome sequencing analysis in a cohort of 52 patients with DLBCL and found no mutations in PIM1 (Fig. 1D). These results suggest that, in addition to PIM1 mutations, its abundance might also play a key role in DLBCL. The COSMIC database indicates that the existing 11 lymphoma cell lines have no PIM1 mutations. To further explore the role of PIM1 in DLBCL, we used three DLBCL cell lines (SU-DHL-8, SU-DHL-2, and Farage) to carry out experiments. A loss-of-function analysis of PIM1 was conducted in these cells by transfection with siRNAs targeting PIM1. PIM1 knockdown significantly suppressed DLBCL cell proliferation (Fig. 1E, F). Collectively, these results establish a rationale for the study of PIM1 as a tumor-dependent factor in DLBCL.

Candidate compound screening for PIM1

To modulate the function of PIM1 in DLBCL, we screened various agents for their potential effects on PIM1 activity. Using the SymMap database, we searched for active compounds that corresponded to PIM1 as a target. These results indicated that Schisandra sphenanthera Rehd. et Wils is a promising compound that can bind to PIM1. Seven lignans are reportedly the main effective components of S. sphenanthera [12]. In this study, we compared the inhibitory effects of seven S. sphenanthera lignans on DLBCL proliferation. Among the lignans, anwulignan showed the best inhibitory effect on DLBCL cells (Fig. 2A). We used the AutoDock Vina software to perform molecular docking of PIM1 with the active component of anwulignan. The docking combinations showed binding energies of –6.4 kcal/mol (Fig. 2B). Therefore, drug affinity-responsive target stability (DARTS) and cellular thermal shift assays (CETSA) were used to confirm the direct interaction between anwulignan and PIM1. These results indicate that anwulignan could directly bind to PIM1(Fig. 2C, D), suggesting that it could be a potential candidate compound for DLBCL treatment by targeting PIM1.

Anwulignan exerts antitumor effects on DLBCL

Anwulignan is a natural compound belonging to the ligand family with a molecular weight of 328.406 Da (Fig. 3A). To investigate the effect of anwulignan on DLBCL cells, three cell lines, SU-DHL-8, SU-DHL-2, and Farage, were treated with different concentrations of anwulignan (3.125, 6.25, 12.5, 25, 50, and 100 μM) for 48 h. Anwulignan dose-dependently inhibited DLBCL cell growth with an inhibitory concentration (IC_{50}) of 60.55 μM against SU-DHL-8, 80.19 μM against SU-DHL-2, and 89.79 μM against Farage (Fig. 3B). In addition, high PIM1 expression correlated with increased sensitivity to anwulignan (Fig. 3C). The anti-proliferative effect of anwulignan was consistent across the DLBCL cell lines tested. Moreover, the cell cycle analysis indicated that anwulignan-induced DLBCL cell cycle arrest occurred at the G0/G1 phase (Fig. 3D). Annexin V/7-AAD staining and Hoechst 33,258 staining showed that anwulignan significantly induced apoptosis in DLBCL cells (Fig. 3E, F). In an animal xenograft model, treatment with anwulignan inhibited tumor growth compared to that in the vehicle-treated group without any significant change in mouse body weight, indicating good tolerance to anwulignan treatment (Fig. 3G, H). These findings suggest that anwulignan exerts potent anti-DLBCL activity in vitro and in vivo by inhibiting DLBCL cell proliferation and inducing apoptosis, indicating its potential as a therapeutic agent for DLBCL.

Anwulignan inhibits DLBCL cell proliferation by targeting the PIM1-c-Myc pathway

To investigate the effect of anwulignan on DLBCL cells, we conducted a comprehensive analysis of the whole transcriptome using RNA sequencing (RNAseq). The heat map shows the

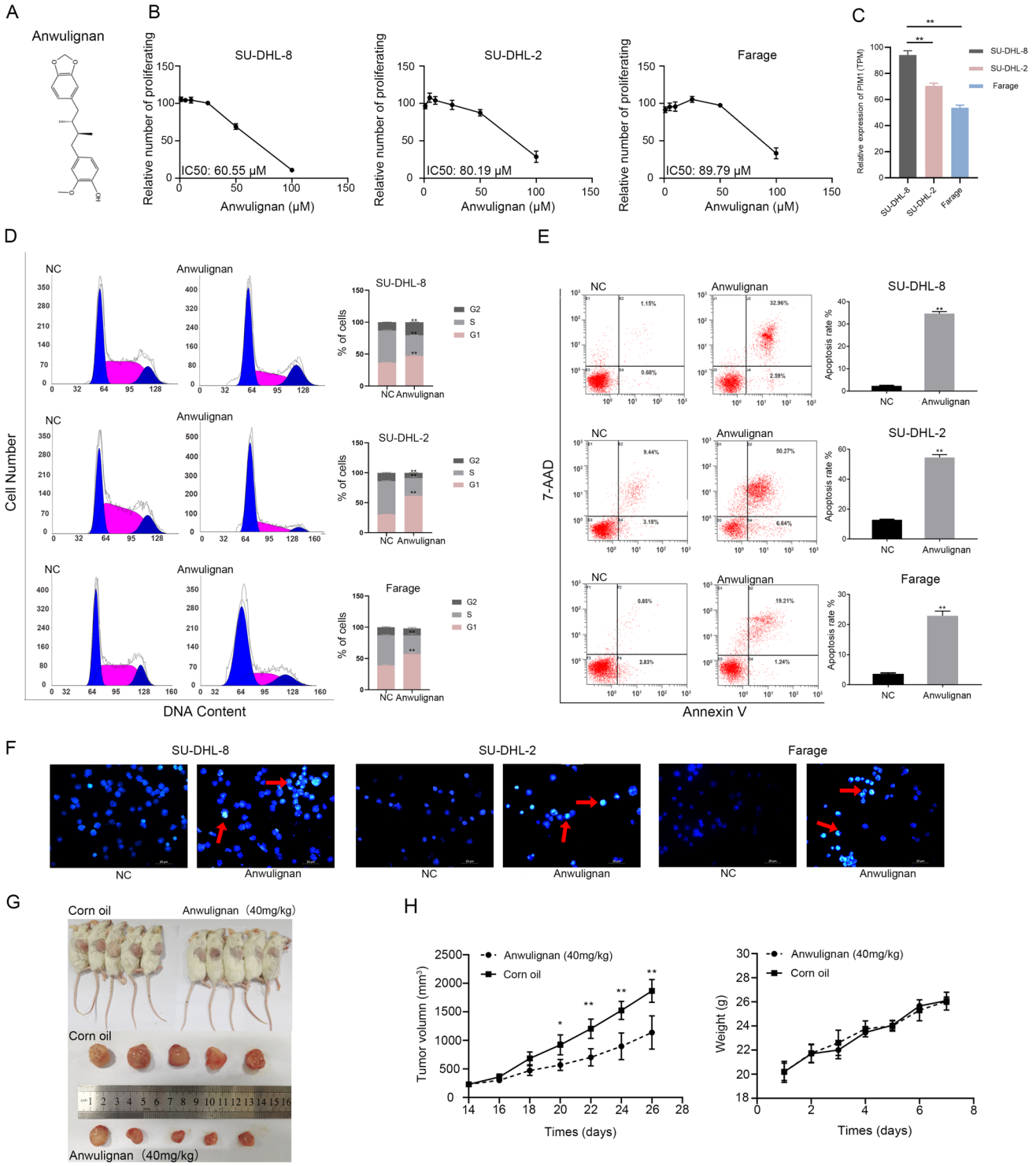

cluster analysis of the DEGs affected by anwulignan (Fig. 4A). Gene Ontology functional annotations demonstrated that genes affected by anwulignan predominantly participated in cell cycle regulation and DNA repair mechanisms (Fig. 4B). Furthermore, KEGG analysis revealed that the cell cycle and DNA replication pathways were critical functional categories that governed the response of DLBCL cells to anwulignan treatment (Fig. 4C). Gene set enrichment analysis (GSEA) revealed transcripts associated with anwulignan were significantly enriched in genes involved in NFκB, MTOR, and c-Myc signaling (Fig. 4D). Collectively, our findings suggest that anwulignan has a wide-ranging impact on the biological processes in DLBCL.

PIM1 is a member of the PIM family of serine/threonine kinase-transforming oncogenes. Studies have shown that

◂**Fig. 3** Anwulignan suppresses the growth and proliferation of DLBCL cells. **A** Chemical structure of anwulignan. **B** DLBCL cell lines (SU-DHL-8, SU-DHL-2, and Farage) were treated with increasing concentrations of anwulignan for 48 h and cell viability was measured by CCK8 assay. IC_{50} values in three different cell lines are shown. **C** The expression level of PIM1 was detected by RNAseq (GSE229896). **D**. SU-DHL-8, SU-DHL-2, and Farage cells were treated with anwulignan (IC_{50}) for 48 h. A Cell cycle phase distribution was determined by flow cytometry. **E** Quantification of cell apoptosis following Annexin V/7-AAD staining. **F** Hoechst 33,258 staining was utilized to examine cell nuclear alterations, which were subsequently visualized under a fluorescence microscope (×200). **G** Subcutaneous injection of SU-DHL-8 cells (1×10^7) was performed in the upper flank of 4-week-old male nude mice. After tumor formation, mice were administered 40 mg/kg anwulignan or vehicle via intraperitoneal injection for 14 days. Tumor samples were collected and imaged using a high-definition digital camera. **H** The tumor volume was assessed on day 14, and the body weight of each mouse was measured every other day. The data are presented as mean ± S.D. of triplicate measurements. Statistical significance was considered at $^*P<0.05$ and $^{**}P<0.01$

inhibition of PIM1 activity downregulates c-Myc phosphorylation at Ser62 [13, 14]. Next, we investigated whether anwulignan could inhibit the phosphorylation of c-Myc by targeting PIM1 in DLBCL. Tryptophan phosphorylation at position 62 was reduced in anwulignan-treated DLBCL cells (Fig. 4E). These results suggested that anwulignan decreased c-Myc activation by targeting PIM1, thus inhibiting the proliferation of DLBCL cells.

Anwulignan induces autophagic cell death in DLBCL cells

GSEA revealed that the expression pattern of MTOR pathway genes was significantly different between the anwulignan and control groups (Fig. 4D, Table S3, Table S4). Since MTOR signaling is a key regulator of autophagy [15], we investigated whether anwulignan treatment could induce autophagic death in DLBCL cells. To evaluate autophagy, we assessed the transformation of LC3I to LC3II, which is a hallmark of autophagy [16]. Immunofluorescence (IF) staining showed a significant accumulation of LC3II in DLBCL cells treated with anwulignan (Fig. 5A). The immunoblotting analysis further confirmed the induction of autophagy by anwulignan, as indicated by an increase in the LC3II/LC3I ratio in treated cells. P62 is another widely used marker for monitoring autophagy, and we found a decrease in P62 expression in DLBCL cells after treatment with anwulignan (Fig. 5B). Next, we used 3-MA, a selective PI3K inhibitor that impedes autophagosome formation, to confirm that anwulignan induces autophagy in DLBCL cells. Co-treatment with anwulignan and 3-MA resulted in the reversal of anwulignan-induced autophagy, as evidenced by the decreased expression of LC3II and increased expression of P62 (Fig. 5C). Moreover, 3-MA partially rescued anwulignan-induced inhibition of cell growth (Fig. 5D). These results suggest autophagy-mediated anti-DLBCL effects of anwulignan.

Synergistic cytotoxicity of anwulignan and chidamide in DLBCL

Single-target therapies for cancer have limited clinical success, whereas combination therapy with two or more targeted drugs has the potential to improve efficacy [17]. To identify effective synergistic combination drugs, we chose four small-molecule drugs that are currently under preclinical and clinical investigation for the treatment of various cancers. IC_{50} values of the drugs (ibrutinib, KPT-330, decitabine, and chidamide) on SU-DHL-8 cells were 11.30 μM, 1.86 μM, 87.61 μM, and 676.80 nM, respectively (Fig. 6A). Next, SU-DHL-8 cells were treated with anwulignan and each of the four agents separately. The combination of anwulignan and chidamide demonstrated potent synergistic cytotoxicity in SU-DHL-8 cells. We investigated the synergistic effects of the two drugs on two other DLBCL cell lines. The IC_{50} values of chidamide for SU-DHL-2 and Farage were 1.71 μM and 7.02 μM, respectively (Fig. 6B). Quantitative analysis of the results revealed that the combination index values were predominantly less than 1.0 in both DLBCL cell lines, indicating a synergistic effect between anwulignan and chidamide (Fig. 6C). Overall, these findings suggest that combining anwulignan with chidamide may be a promising strategy for improving the therapeutic efficacy of chidamide in clinical settings.

Discussion

In the present study, we conducted a screening and identified anwulignan as a potent natural compound with anti-DLBCL activity. Anwulignan inhibits the proliferation of DLBCL cells by decreasing the activation of c-Myc by targeting PIM1. Moreover, anwulignan synergistically enhanced the effects of chidamide on DLBCL. Our data suggest that anwulignan is a promising natural compound for the treatment of DLBCL.

Over the past two decades, the prevalence of DLBCL has increased annually. Although first-line treatment with R-CHOP has substantially improved outcomes for patients with DLBCL, approximately 40% of patients still experience relapsed/refractory disease with poor survival outcomes [18]. Creating new treatments for DLBCL, particularly using natural sources, is viewed as a crucial approach. Our research showed that PIM1 plays a crucial role in the proliferation of DLBCL cells and that its high expression is associated with poor survival in patients with DLBCL.

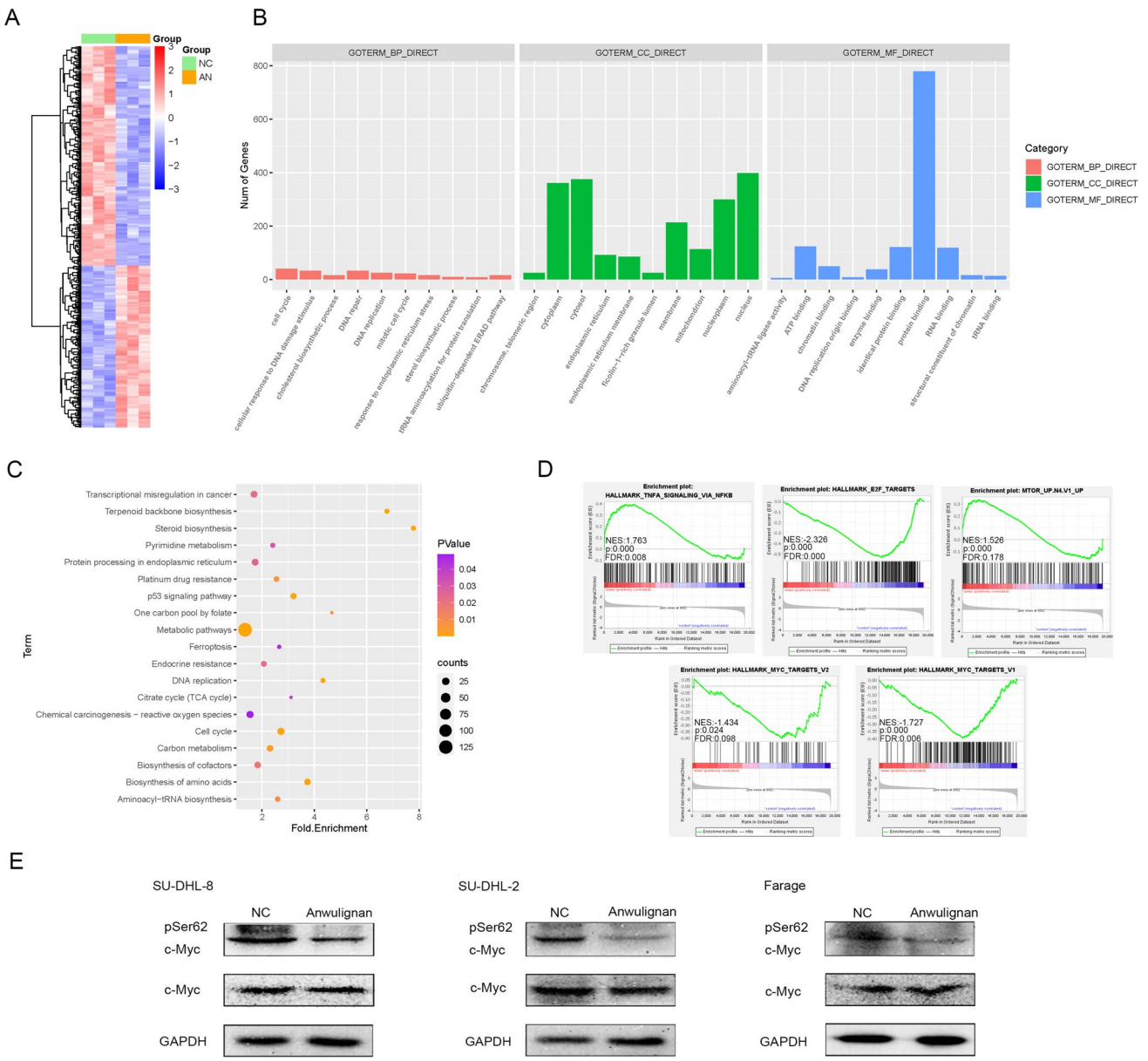

Fig. 4 Effect of anwulignan on the transcriptome in DLBCL cells. **A** The mRNA expression values are presented in a color gradient from dark red, indicating the highest expression, to dark blue, representing the lowest. **B** The top 10 entries for biological process, molecular function, and cell composition (based on FDR < 0.05) are displayed to represent the distribution of GO entries. Darker shades of color indicate higher significance levels. **C** The 19 most significant KEGG pathways are displayed, with the size of each dot representing the number of corresponding genes and the color scale indicating the p-value threshold. **D** Detailed enrichment plot of the Hallmark TNFA SIGNALING VIA NFKB, E2F TARGETS, MTOR, and MYC TARGETS pathway. **E** After 48 h of treatment with anwulignan (IC_{50}), the protein extracts from the SU-DHL-8, SU-DHL-2, and Farage cells were analyzed by western blotting to determine the changes in the levels of c-Myc and pSer62 c-Myc proteins

These findings demonstrate the oncogenic functions of PIM1 in DLBCL cells and support the development of small-molecule PIM inhibitors and targeted therapies for PIM kinases in lymphomas.

Natural products and their analogs are important components of pharmacotherapy, especially for the treatment of cancer [8, 9]. However, their applications are often limited by a lack of understanding of their targets. Screening natural compound libraries identified anwulignan as a promising compound that binds to PIM1 and shows potential against DLBCL. Anwulignan was extracted from Schisandra sphenanthera Rehd. et Wils, and previously demonstrated anti-non-small cell lung cancer activity [19]. Our findings indicate that anwulignan exerts noteworthy anti-DLBCL activity by

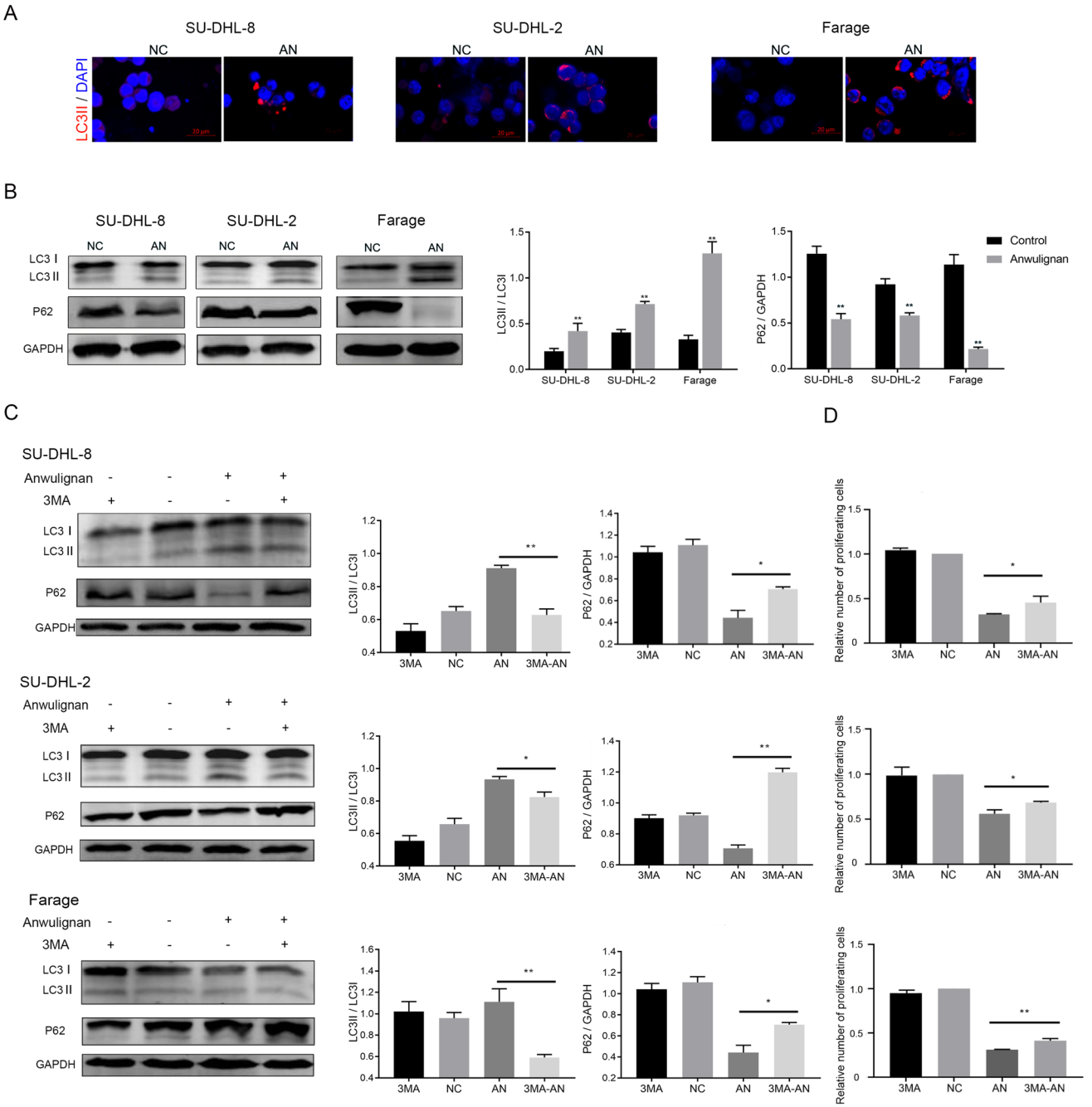

Fig. 5 Anwulignan induces autophagic cell death in DLBCL cells. **A** The genes that exhibited differential expression between the control and anwulignan groups were primarily enriched in MTOR-related pathways. Enrichment was considered significant at FDR < 0.25 and $P < 0.05$. Normalized enrichment score (NES) and false discovery rate (FDR) were also calculated. **B** SU-DHL-8, SU-DHL-2, and Farage cells were treated with varying concentrations of anwulignan for 24 h. LC3II puncta formation was then analyzed using immunofluorescence and visualized using confocal microscopy. **C** SU-DHL-8, SU-DHL-2, and Farage cells were treated with anwulignan at the indicated concentration for 24 h. LC3II and P62 were determined by immunoblotting. **D** SU-DHL-8, SU-DHL-2, and Farage cells were treated with anwulignan for 24 h in the absence or presence of 3-MA (5 mM). LC3II and P62 were determined by immunoblotting. E SU-DHL-8, SU-DHL-2, and Farage cells were treated with anwulignan at the indicated concentration for 24 h in the absence or presence of 3-MA (5 mM), and cell viability was detected by CCK-8 assay. All data are shown as the means ± S.D. based on triplicate measures; $^{*}P < 0.05$ and $^{**}P < 0.01$

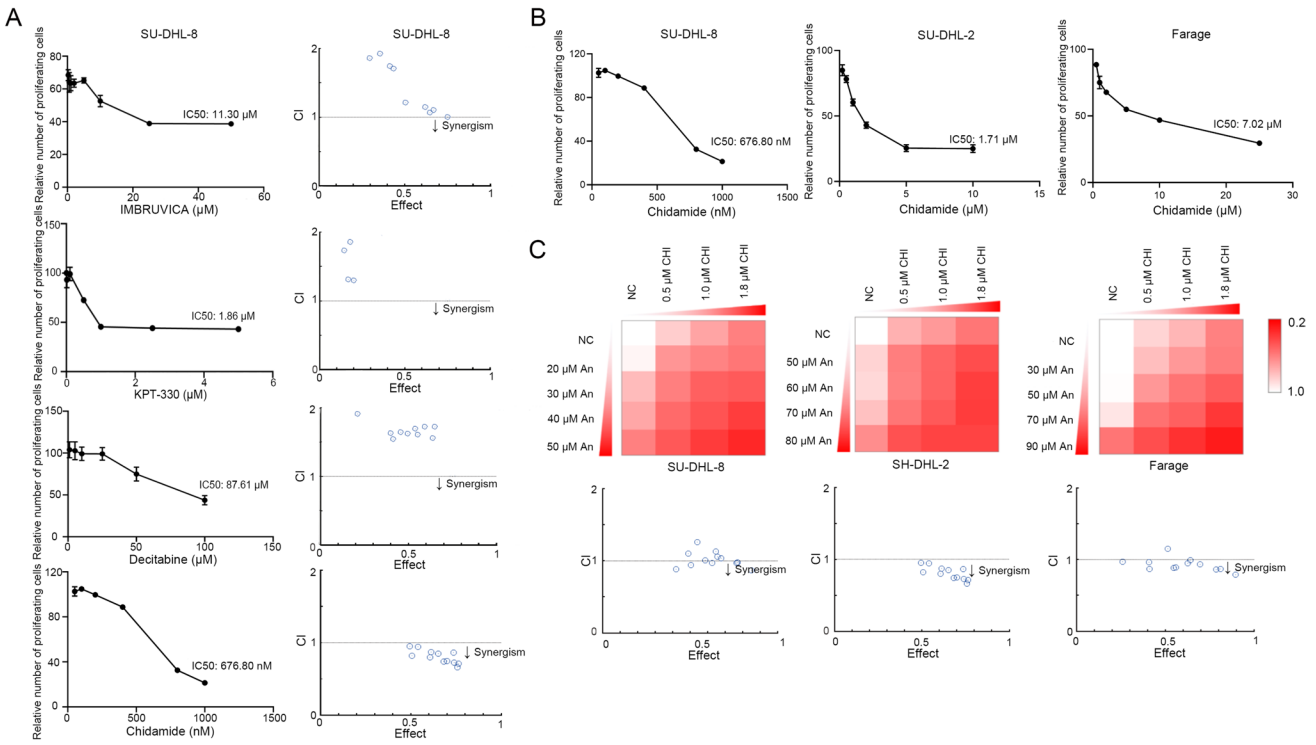

Fig. 6 Anwulignan synergizes Chidamide-mediated cytotoxicity. **A** SU-DHL-8 cell line was treated with increasing concentrations of ibrutinib, KPT-330, decitabine, and chidamide for 48 h and cell viability was measured by CCK8 assay. IC_{50} values in the SU-DHL-8 cell line are shown. **B** DLBCL cell lines (SU-DHL-8, SU-DHL-2, and Farage) were treated with increasing concentrations of chidamide for 48 h and cell viability was measured by CCK8 assay. IC_{50} values in two cell lines are shown. **C** The CI values were calculated using CompuSyn software based on the Chou-Talalay equation, and the results were plotted as CI symbols at twelve different dose points for each Fa

suppressing cell proliferation and promoting apoptosis. Over the past few years, the DARTS assay and CETSA have been instrumental in identifying and uncovering targets of small molecules [20, 21]. Using both approaches, we verified that anwulignan can bind to PIM1. PIM1 belongs to the PIM family of serine/threonine kinase-transforming oncogenes, which regulate multiple pro-survival pathways and cooperate with other oncogenes such as c-Myc [7]. Studies have shown that the inhibition of PIM1 activity downregulates c-Myc phosphorylation at Ser62, resulting in a significant reduction in the oncogenicity of c-Myc. Abnormal c-Myc activity has been reported in different types of cancer, including DLBCL [22]. Decreased c-Myc activity slows cell cycle progression, suppresses DLBCL cell proliferation, and induces a substantial level of apoptosis both in vitro and in vivo [23]. Our data indicate that anwulignan is a specific inhibitor of PIM1 that directly binds to PIM1 and induces DLBCL cell death via c-Myc-dependent mechanisms. In addition, we found that anwulignan could induce autophagy in DLBCL cells. However, it was unclear at the time whether the autophagic induction by anwulignan was associated with PIM1, and further research was needed to clarify this relationship.

Interestingly, anwulignan exhibited a synergistic effect with chidamide. Studies have indicated that chidamide can promote cell apoptosis by downregulating c-myc expression [24, 25], and our research revealed that anwulignan could induce apoptosis in DLBCL cells by inhibiting the phosphorylation of c-myc without affecting its expression. Therefore, we hypothesize that the two compounds may complement each other, inhibiting both the expression and function of c-myc, thereby exerting a synergistic effect.

Overall, our findings suggest that anwulignan holds great promise as a therapeutic agent for DLBCL.

Supplementary Information The online version contains supplementary material available at https://doi.org/10.1007/s00277-024-05670-7.

Author contribution Wenzhuo Zhuang and Bingzong Li designed the research, Xinyun Zhang and Qi Su performed research, Xinyun Zhang wrote the paper, Rong Rong, Si Chen and Lexin He performed research and modified the paper, Yuchen Zhang analyzed data.

Funding This work was supported by the Natural Science Foundation of China (82270197, 82270211), The special project of "Technological innovation" project of CNNC Medical Industry Co. Ltd (ZHYLYB2021002), Natural Science Foundation of Jiangsu Province China (BK20201408).

Data availability The data supporting the findings of this study can be found in the article or available from the corresponding author upon reasonable request.

Declarations

Ethical approval The animal experimentation acquired permission from the ethics committee of Soochow university. The study was conducted in accordance with the Declaration of Helsinki.

Competing interests The authors declare that they have no competing interests.

References

1. Alizadeh AA, Eisen MB, Davis RE et al (2000) Distinct types of diffuse large B-cell lymphoma identified by gene expression profiling. Nature 403(6769):503–511
2. Chen H, Qin Y, Liu P et al (2023) Genetic profiling of diffuse large B-cell lymphoma: a comparison between double-expressor lymphoma and non-double-expressor lymphoma. Mol Diagn Ther 27(1):75–86
3. Wang L, Li LR (2020) R-CHOP resistance in diffuse large B-cell lymphoma: biological and molecular mechanisms. Chin Med J (Engl) 134(3):253–260
4. Panchal NK, Sabina EP (2020) A serine/threonine protein PIM kinase as a biomarker of cancer and a target for anti-tumor therapy. Life Sci 255:117866
5. Szydłowski M, Prochorec-Sobieszek M, Szumera-Ciećkiewicz A et al (2017) Expression of PIM kinases in Reed-Sternberg cells fosters immune privilege and tumor cell survival in Hodgkin lymphoma. Blood 130(12):1418–1429
6. Chen LS, Redkar S, Bearss D, Wierda WG, Gandhi V (2009) Pim kinase inhibitor, SGI-1776, induces apoptosis in chronic lymphocytic leukemia cells. Blood 114(19):4150–4157
7. Szydłowski M, Garbicz F, Jabłońska E et al (2021) Inhibition of PIM Kinases in DLBCL targets MYC transcriptional program and augments the efficacy of anti-CD20 antibodies. Cancer Res 81(23):6029–6043
8. Spradlin JN, Hu X, Ward CC et al (2019) Harnessing the anticancer natural product nimbolide for targeted protein degradation. Nat Chem Biol 15(7):747–755
9. Yarla NS, Bishayee A, Sethi G et al (2016) Targeting arachidonic acid pathway by natural products for cancer prevention and therapy. Semin Cancer Biol 40–41:48–81
10. Kampan NC, Madondo MT, McNally OM, Quinn M, Plebanski M (2015) Paclitaxel and its evolving role in the management of ovarian cancer. Biomed Res Int 2015:413076
11. Hartert KT, Wenzl K, Krull JE et al (2021) Targeting of inflammatory pathways with R2CHOP in high-risk DLBCL. Leukemia 35(2):522–533
12. Lu Y, Chen DF (2009) Analysis of Schisandra chinensis and Schisandra sphenanthera. J Chromatogr A 1216(11):1980–1990
13. Horiuchi D, Camarda R, Zhou AY et al (2016) PIM1 kinase inhibition as a targeted therapy against triple-negative breast tumors with elevated MYC expression. Nat Med 22(11):1321–1329
14. Zhang Y, Wang Z, Li X, Magnuson NS (2008) Pim kinase-dependent inhibition of c-Myc degradation. Oncogene 27(35):4809–4819
15. Kim YC, Guan KL (2015) mTOR: a pharmacologic target for autophagy regulation. J Clin Invest 125(1):25–32
16. Kabeya Y, Mizushima N, Ueno T et al (2000) LC3, a mammalian homologue of yeast Apg8p, is localized in autophagosome membranes after processing. Embo J 19(21):5720–5728
17. Colli LM, Machiela MJ, Zhang H et al (2017) Landscape of combination immunotherapy and targeted therapy to improve cancer management. Cancer Res 77(13):3666–3671
18. Poletto S, Novo M, Paruzzo L, Frascione PMM, Vitolo U (2022) Treatment strategies for patients with diffuse large B-cell lymphoma. Cancer Treat Rev 110:102443
19. Xie X, Wang X, Shi X et al (2021) Anwulignan is a novel JAK1 inhibitor that suppresses non-small cell lung cancer growth. J Cell Mol Med 25(5):2645–2654
20. Skrott Z, Mistrik M, Andersen KK et al (2017) Alcohol-abuse drug disulfiram targets cancer via p97 segregase adaptor NPL4. Nature 552(7684):194–199
21. Ross NT, Lohmann F, Carbonneau S et al (2020) CPSF3-dependent pre-mRNA processing as a druggable node in AML and Ewing's sarcoma. Nat Chem Biol 16(1):50–59
22. Buettner R, Morales C, Caserta E et al (2019) Leflunomide regulates c-Myc expression in myeloma cells through PIM targeting. Blood Adv 3(7):1027–1032
23. Kreuz S, Holmes KB, Tooze RM, Lefevre PF (2015) Loss of PIM2 enhances the anti-proliferative effect of the pan-PIM kinase inhibitor AZD1208 in non-Hodgkin lymphomas. Mol Cancer 14:205
24. Gu S, Hou Y, Dovat K, Dovat S, Song C, Ge Z (2023) Synergistic effect of HDAC inhibitor chidamide with cladribine on cell cycle arrest and apoptosis by targeting HDAC2/c-Myc/RCC1 axis in acute myeloid leukemia. Exp Hematol Oncol 12(1):23
25. Luo C, Yu T, Young KH, Yu L (2022) HDAC inhibitor chidamide synergizes with venetoclax to inhibit the growth of diffuse large B-cell lymphoma via down-regulation of MYC, BCL2, and TP53 expression. J Zhejiang Univ Sci B 23(8):666–681